Sliding-Mode Observer based Direct Torque Control of an IPM-Synchronous Motor Drive at Very Low Speed

Vaishali Chandrakant Chormare[1], Subhash S. Sankeshwari[2]

[1]*Control System, MBES College of engineering and Technology, Ambajogai.*
[2]*Assistant Professor and Head of Electrical, Electronics and Power Engineering Department in M.B.E.S's college of engineering Ambajogai, India*

Abstract: *Fast torque and flux dynamic responses are delivered by direct torque control of interior permanent-magnet synchronous motors. However, the major drawback is being the poor flux estimation at very low speeds. A majority of flux observers have been proposed for flux estimation, but most of them fail to check in the low-speed region. In this paper, to improve flux estimation at very low speeds, a sliding-mode stator flux observer is proposed. This observer does not require any speed adaptation mechanism unlike conventional flux observers and is immune to speed estimation error. A novel stator resistance estimator is incorporated into the sensor less drive to compensate the effects of stator resistance variation. DC-offset effects are reduced by introducing a small elemental component in the observer gains. Simulation results at very low speeds, including 0 and 2 r/min, without signal injection confirm the effectiveness of the proposed method.*

Keywords:
1. Active flux
2. direct torque control (dtc)
3. Interior permanent-magnet synchronous motor (ipmsm)
4. sliding-mode
5. Flux observer

Nomenclature

|	
$i = (i_\alpha \quad i_\beta)^T$	Stator current in the $\alpha\beta$ reference frame.
i_d, i_q	Stator current in the dq reference frame.
$\tilde{i} = (\tilde{i}_\alpha \quad \tilde{i}_\beta)^T$	Stator current estimation error
I	$=\begin{pmatrix} 1 & 0 \\ 0 & 1 \end{pmatrix}$
J	$=\begin{pmatrix} 0 & -1 \\ 1 & 0 \end{pmatrix}$
L	$=\begin{pmatrix} Ld & 0 \\ 0 & Lq \end{pmatrix}$
L_d, L_q	dq-axes inductances
R_s	Stator Resistance
T	Electromagnetic Torque
$V=(V_\alpha \quad V_\beta)^T$	Stator Voltage in the $\alpha\beta$ reference frame
V_d, V_q	Stator Voltage in the dq reference frame
θ_{re}	Rotor angle
$\lambda = (\lambda_\alpha \quad \lambda_\beta)^T$	Stator flux linkage in the $\alpha\beta$ reference frame
λ_d, λ_q	Stator flux linkage in the dq reference frame
λ_f	Permanent magnetic flux linkage
$\tilde{\lambda} = (\tilde{\lambda}_\alpha \quad \tilde{\lambda}_\beta)^T$	Stator flux estimation error.
ω_{re}	Rotor speed
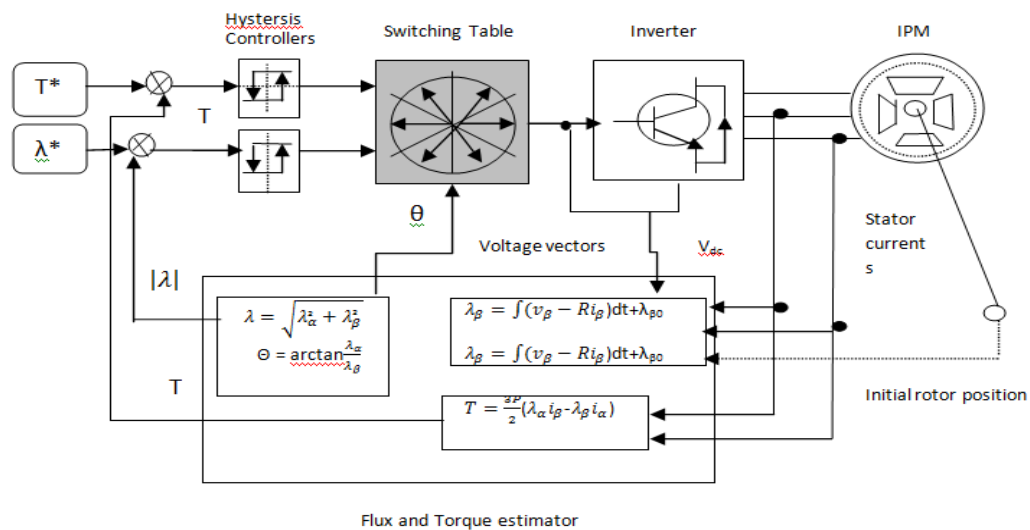
Fig.1 Block Diagram Of The Dtc.

I. Introduction

Direct Torque Control: (DTC) is one method used in variable frequency drives to control the torque. This involves calculating an estimate of the motor's magnetic flux and torque based on the measured voltage and current of the motor. DTC was patented by Manfred Depenbrock in the US and in Germany. However, Isao Takahashi and Toshihiko Noguchi described a similar control technique termed DTC in an IEEJ paper presented in September 1984 and in an IEEE paper published in late 1986. The DTC innovation is thus usually credited to all three individuals. Since its mid-1980s introduction applications, DTC have been used to advantage because of its simplicity and very fast torque and flux control response for high performance induction motor (IM) drive applications. DTC techniques for the interior permanent magnet synchronous machine (IPMSM) were introduced in the late 1990s.There are many advantages of direct torque control when compared to conventional vector-controlled drives, such as elimination of coordinate transformation, lesser parameter dependence, and faster dynamic response [3].

DTC results fast responses, as the torque and flux are regulated directly and independently. Additionally, due to the absence of coordinate transformation, DTC is intrinsically sensorless. The main disadvantage is the inability to estimate the stator flux at low speeds precisely. Usage of an encoder for stable operation at low speeds seems to disprove the benefits of the DTC. Furthermore, the cost of the DTC increases due to the existence of this position sensor at the same time reducing the reliability of the system.

The several solutions that have been proposed by many researchers to this problem are classified as follows:

- Open-loop back-EMF-based estimators [3]–[6];
- Closed-loop adaptive observers based on advanced models [7]–[16];
- Estimation based on high-frequency signal injection, exploiting the saliency property of an IPMSM [17]–[23].

Every solution has its own advantages and disadvantages and most of them (except the latter) fail to deliver efficient performance at very low speeds. The signal injection methods allow sensorless operation at standstill, even then there will be increase in the noise in the system resulting in reduced overall efficiency. Moreover, when this method is endorsed for sensorless control, the gesture of the system are shown to be stagnant.

In this paper, a novel sliding-mode stator flux observer is proposed that has the capability of estimating accurate flux at very low speeds without signal injection. Since the concept of active flux was used by this observer the sensorless control could able to perform in a simpler way on an IPM machine. As the active flux is adopted, the proposed observer can be implemented in a dual reference frame which in turn allows it to be inherently sensorless. No speed adaption mechanism is required by the observer and thus, any inexactness due to speed estimation errors is eliminated [27]. This extremely improves the flux estimation at very low speed. Regardless, the effects of dc-measurement offset parameter variations were not taken into account as they pose significant problems at very low speeds. Furthermore, the observer gains selection, which may become critical at very low speeds, were not elaborated.

The proposed sliding-mode flux observer in this paper is superior to that in [28]. To alleviate any effect of stator resistance variation at low speed, an online stator resistance estimator is integrated into the proposed flux observer. In the proposed observer the effect of variations in L_q is accounted for by the sliding-mode term.

The observer gains selection procedure is also included. At low speeds, to overcome the undesirable effects of dc-measurement offset, an integral component is combined with the observer gain. Simulation results of the sensorless DTC drive at very low speeds, including standstill and 2r/min, are included to verify the effectiveness of the proposed approach.

II. Sliding-Mode Observer (Smo)

The performance of a sensorless drive is affected by the accuracy of the stator flux observer which is a key factor. In the stationary (αβ) or rotating frame (dq) the adaptive observers are commonly used because of its robustness towards disturbance rejection and parameter variations. However, these observers are always realized in a single reference frame that results in a rotor-speed-dependant term. Therefore, the observer has to be speed adaptive and the speed adaptation is usually performed as the last step of the estimation process in a digital realization. Hence, the speed estimate is affected by cumulative errors, noise, and delays. The flux and speed estimation gradually worsen when the inaccurate speed value is fed back to the observer. This can easily lead the drive to instability, especially, at low speeds.

A. Design Of The Observer

If both the rotating (dq) and stationary (αβ) frames are used the speed dependency term can be eliminated. Defining the stator flux as the state variable and the stator current as the output, a closed-loop SMO without speed adaptation can be designed which is shown in Fig. 2. Depending upon the machine equations in the rotor (dq) reference
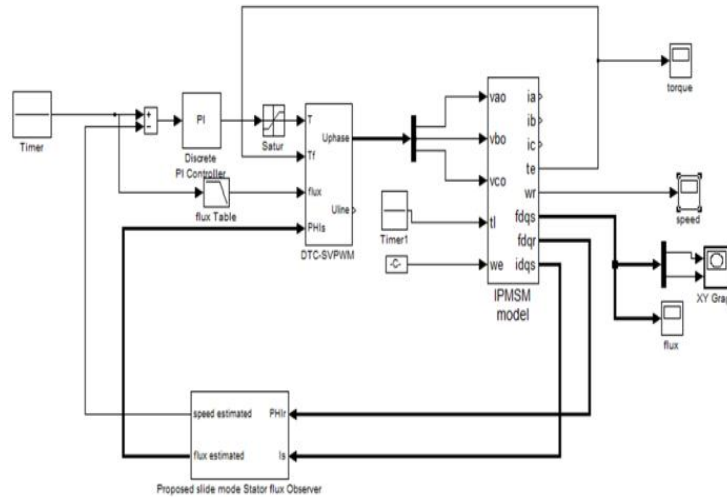

Fig.2. Block Diagram Of The Proposed Sliding-Mode Stator Flux Observer.

Frame, the stator flux observer can be mathematically expressed as follows:

$$\frac{d}{dt}\hat{\lambda} = -\hat{r}_s i + v + k\tilde{i} + k_{smo}\,\text{sign}(\tilde{i})$$

$$\hat{I} = t^{-1}(\hat{\theta}_{re})\,l^{-1}\,t\,(\hat{\theta}_{re})\hat{\lambda} + \frac{\lambda_f}{L_d}\begin{pmatrix} \cos\hat{\theta}_{re} \\ -\sin\hat{\theta}_{re} \end{pmatrix} \qquad (1)$$

$$\text{Where} \qquad t(\hat{\theta}_{re}) = \begin{pmatrix} \cos\hat{\theta}_{re} & -\sin\hat{\theta}_{re} \\ \sin\hat{\theta}_{re} & \cos\hat{\theta}_{re} \end{pmatrix}$$

K and k_{smo} are the observer gains, and ^ denotes the estimated quantities. The observer employs both linear and nonlinear feedback terms. The error dynamics and robustness are determined by the linear and nonlinear gains, respectively. The estimated rotor angle is calculated from

$$\hat{\theta}_{re} = \tan^{-1}\left(\frac{\hat{\lambda}_{a,\beta}}{\hat{\lambda}_{\alpha,\alpha}}\right) \qquad \textbf{(2)}$$

$$\text{Where} \qquad \begin{cases} \hat{\lambda}_{a,\alpha} = \hat{\lambda}_\alpha - L_q i_\alpha \\ \hat{\lambda}_{a,\beta} = \hat{\lambda}_\beta - L_q i_\beta \end{cases} \qquad \textbf{(3)}$$

Is called the active flux [24]–[26]. The observer employs two reference frames—both the stationary (αβ) and rotor (dq) frames. To estimate the stator flux the voltage model is implemented by the state equation in the stationary (αβ) frame. Based on (2) and (3) the active flux and estimated rotor position are calculated. Using the current model, the output equation of the observer estimates the current, assuming orientation. The current

estimation errors are then used as feedback signals for correction. The stator flux observer combines the advantages of the current model at low speeds and that of the voltage model at higher speeds.

B. Observer Gain Selection

The classical approach to observer gain selection is to design the observer poles proportional to the motor poles [9]. This approach allows the observer to be dynamically faster than the motor, but is susceptible to noise. This problem can be circumvented by designing the observer poles with identical imaginary parts as the motor poles, but shifted to the left in the complex plane [10]. This approach is adopted in this paper. The observer still possesses faster dynamics than the machine. Nevertheless,
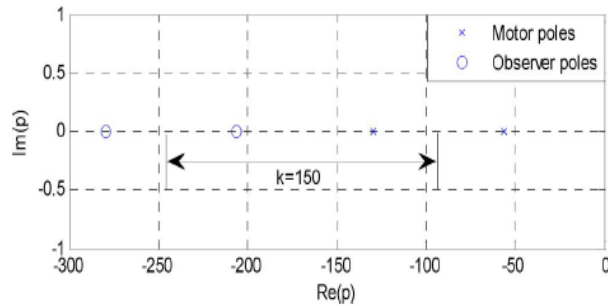

Fig. 3 Location of motor and observer poles for k = 150.

The noise immunity of the observer is improved because the other pole, already having a large magnitude, is less amplified. It can be shown that poles of the machine as a function of rotor speed are given by

$$p_{1,2}(\omega_{re}) = -\frac{R_s}{L_d}, -\frac{R_s}{L_q} \qquad (4)$$

On the other hand, the poles of the observer are governed by the eigen values of $[k_1 i + J (k_2 i - \omega_{re}l)]$ in (10). Shifting the observer poles to the left by k yields

$$p_{o1,2}(\omega_{re}) = -\frac{R_s}{L_d} - k, -\frac{R_s}{L_q} - k \qquad (5)$$

Where k > 0. Imposing this condition on the observer results in the following individual gains k1 and k2 as a function of rotor speed:−

$$\begin{cases} k_1 = \frac{R_s}{2}\left(\frac{1}{L_d} + \frac{1}{L_q}\right) + k \\ k_2 = \frac{1}{2}\{\omega_{re}(L_d + L_q) \\ +\text{sign}(\omega_{re})\left[(L_d - L_q)\sqrt{\omega_{re}^2 - \left(\frac{R_s}{L_d L_q}\right)^2}\right]\} \end{cases} \qquad (6)$$

Since the actual speed ω_{re} is not available, the estimated one is used instead. Fig. 3 illustrates the machine and observer poles in the complex plane for k = 150. On the other hand, Fig. 4 shows the machine and observer poles in the complex plane when constant gains $k_1 = 150$ and $k_2 = 50$ are used instead. It is evident that the imaginary component of the observer poles increases with speed and this induces unwanted oscillations at high speeds.

If $\qquad K_{SMO} = \begin{pmatrix} K_{SMO,1} & 0 \\ 0 & K_{SMO} \end{pmatrix}$

Equation (11) yields

$$K_{SMO,1}\left|\tilde{\iota}_\alpha\right| + K_{SMO,2}\left|\tilde{\iota}_\beta\right| > 0 \qquad (7)$$

Hence, $K_{SMO,1}, K_{SMO,2} > 0$. Fig. 5 depicts the torque and flux estimation errors due to +20% detuning in L_q when $K_{SMO,1} = K_{SMO,2} = 0$. Fig. 6 illustrates smaller estimation errors when the sliding-mode gains$k_{smo,1} = K_{SMO,2} = 0.1$ are inserted. Larger values of $K_{SMO,1}$ and $K_{SMO,2}$ further increase the robustness of the observer,

Fig. 4. Location Of Motor And Observer Poles For Constant Gains $K_1 = 150$, $K_2 = 50$.

Fig. 5. Torque And Flux Estimation Errors Due To +20% Detuning In L_q.

Fig. 6. Torque And Flux Estimation Errors Due To +20% Detuning In L_q And Sliding-Mode Gains $K_{smo,1}$ = $K_{smo,2}$ = 0.1.

But may generate unwanted chattering. $0 < k_{smo,1}, k_{smo,2} < 1$ is practical for a real drive.

Fig. 7. Block Diagram Of The Proposed Sensorless Dtc Scheme.

Table I: Switching Table Of The Classical Dtc

λ	Τ	θ_1	θ_2	θ_3	θ_4	θ_5	θ_6
λ =1	Τ=1	V2(110)	V3(010)	V4(011)	V5(001)	V6(101)	V1(100)
	Τ=0	V6(101)	V1(100)	V2(110)	V3(010)	V4(011)	V5(001)
λ =0	Τ=1	V3(010)	V4(011)	V5(001)	V6(101)	V1(100)	V2(110)
	Τ=0	V5(001)	V6(101)	V1(100)	V2(110)	V3(010)	V4(011)
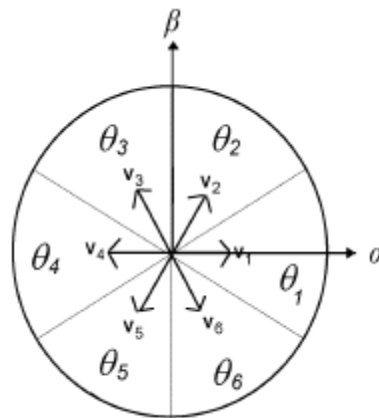
Fig. 8. Regions $\Theta_1 - \Theta_6$ Of The Stator Flux Linkage Vector.

C. Torque And Rotor Speed Estimation

The electromagnetic torque is estimated from

$$\widehat{T} = \frac{3}{2} P(\hat{\lambda}_\alpha i_\beta - \hat{\lambda}_\beta i_\alpha)$$

(8)

The rotor speed is only required for speed control. It can be calculated based on the derivative of (2)

$$\widehat{\omega}_{re} = \frac{\hat{\lambda}_{\alpha,\alpha(k-1)}\hat{\lambda}_{\alpha,\beta(k)} - \hat{\lambda}_{\alpha,\beta(k-1)}\hat{\lambda}_{\alpha,\alpha(k)}}{T_s(\hat{\lambda}^2_{\alpha,\alpha(k)} + \hat{\lambda}^2_{\alpha,\beta(k)})}$$

(9)

where T_s is the sampling period and k and k−1 denote two consecutive sampling instants. The speed signal is low-pass filtered to remove the noise. This is a compact, yet effective, speed estimation scheme.

III. Simulation Results

Simulation using MATLAB/SIMULINK has been done to verify the effectiveness of the proposed sensorless DTC drive scheme. The block diagram of the sensorless drive is shown in Fig. 7. The Table I shows the switching logic of the DTC. Variables λ and τ are the

Table II: Parameters Of IPMSM Used In This Paper

Rated torque	T	6 Nm
Number of poles	P	4
Stator resistance	R_s	5.8 Ω
Magnet flux linkage	λ_f	0.533 Wb
d-axis inductance	L_d	0.0447 H
Phase voltage	V	132 V
Line current	I	3 A
Base speed	ω_b	1500 rpm

Table III: Control Parameters Of The Drive Used In This Paper

K_p for speed controller(Nm.s/rad.)	0.9
K_i for speed controller(Nm.s/rad.)	0.009
Observer pole shift,k	100
Sliding mode gain ϕ_{11}, ϕ_{22}	0.1
Observer integral gain,k_1	0.5
γ for stator resistance estimator	10

Outputs of the flux and torque hysteresis controllers, respectively and $\lambda = 1$ implies that the estimated flux is smaller than its reference value and vice versa. The same thing applies to τ for torque control.

Stator flux vector lies in the region $\theta_1 - \theta_6$, as defined in fig. 8. To carry out the real-time algorithm a ds1104 dsp card was used and for an inverter a three-phase insulated-gate bipolar transistor (igbt) intelligent power module is used. C language was used to code the real-time control software. Ds1104 board generates the pulsewidth modulated (pwm) signals. In simulation, the sampling period of the drive was set to 50 μs.

The armature current of the dc machine is separately regulated and it is used to contend the load. The ipm machine, whose parameters are tabulated in table ii, was used in this simulation. The position signal was solely used for comparison and not for control purposes and to obtain this an incremental encoder was used. To increase the efficiency of the drive system [4] the reference flux value was selected according to the maximum torque per ampere (mtpa) trajectory. Table iii shows the control parameters of the drive. The nonlinearities of the inverter severely affects the performance of the sensorless drive, especially, at low speeds. To sustain very-low-speed sensorless operation, accurate forward voltage drop and dead-time compensation are mandatory [29].

The high-frequency signal injection method [18] was used to estimate the initial rotor position only and not used subsequently for control purposes. The d-axis inductance l_d and the permanent magnet flux λ_f stays relatively constant with variation in operating current. On the other hand, the q-axis inductance l_q decreases as the operating current increases.
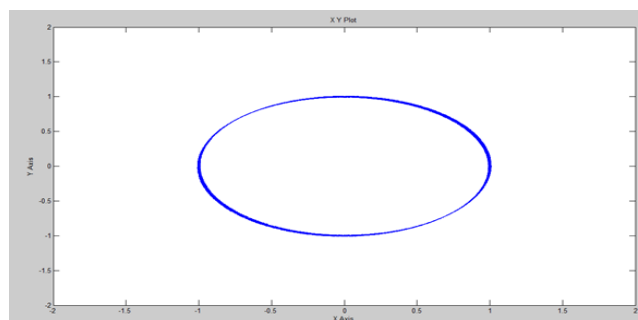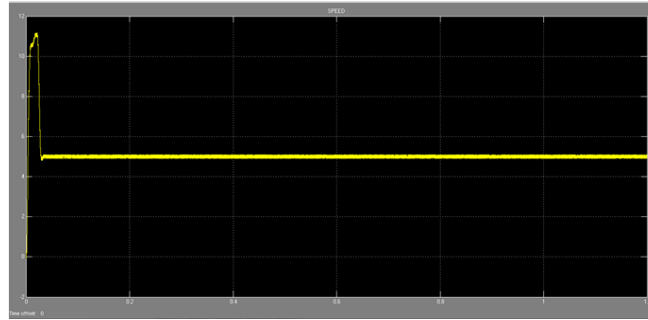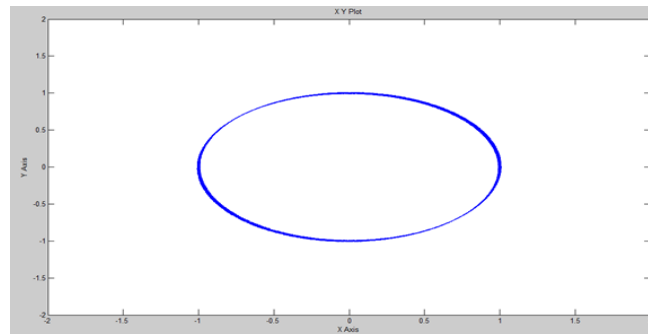

X-Y Plot
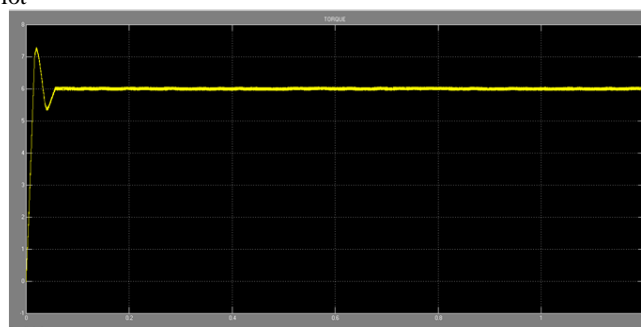
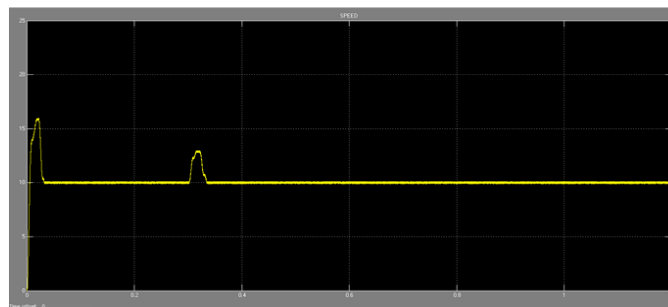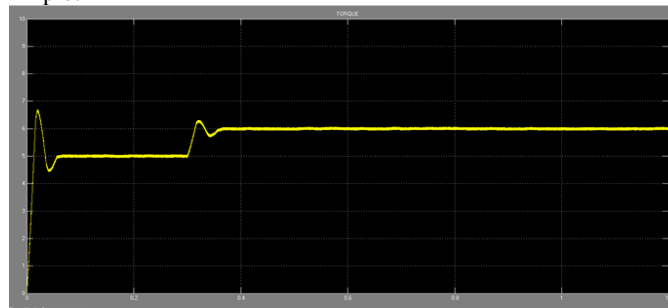**Fig.9. Sensorless Full-Load Operation At 5 R/Min.**

X-Y plot

Fig. 10. Sensorless Full-Load 10 R/Min.

The steady-state operation at 5 r/min with full load is shown in Fig. 9. The same quantities are shown. The speed and torque ripples are now higher, but the system is stable. Low-speed 10 r/min with full load is depicted in Fig. 10. The actual speed, estimated torque and flux, and speed estimation error are shown. The estimated speed follows the actual speed very closely during the transient and steady state. The dynamic response during acceleration from standstill to 2 r/min is shown in Fig. 11. The machine was originally operated at zero speed with no load and was then accelerated to 1000 r/min. The estimated speed tracks the actual speed closely during the transient and steady state.
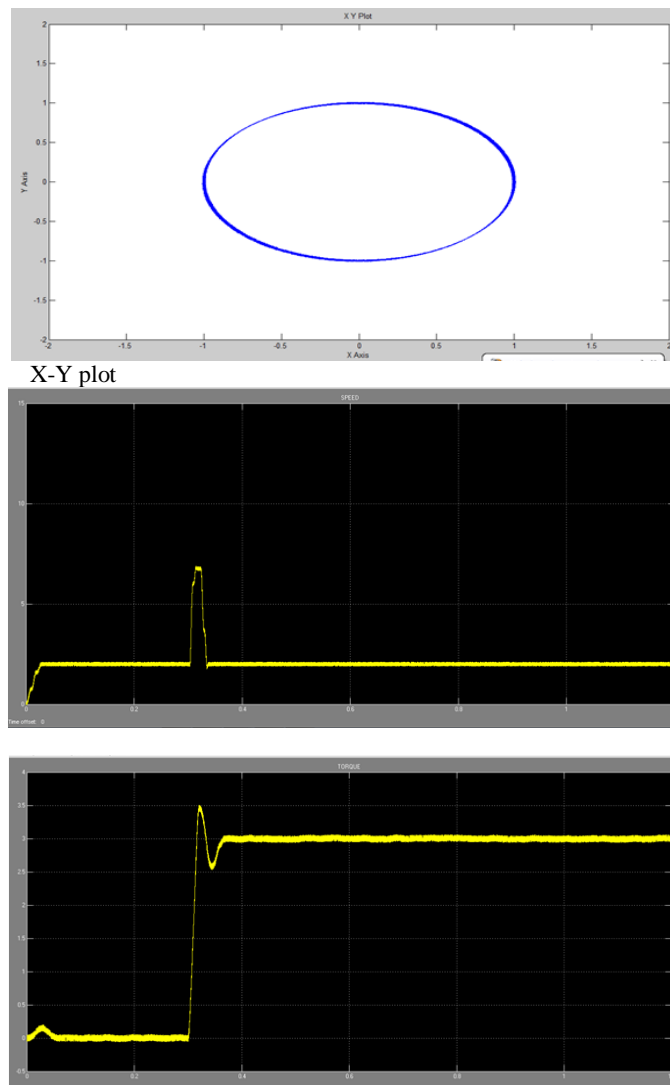
X-Y plot

Fig. 11 Start-Up Response Of The Sensorless Drive.

IV.   Conclusion

In this paper, a sliding-mode stator flux observer for DTC of IPMSM drives was presented. Due to the adoption of the active flux concept, the stator flux observer was implemented in a dual reference frame. As a consequence, it does not require speed adaptation and is not susceptible to speed estimation errors, especially, at low speed. A novel online resistance estimator was proposed to further compensate for the effects of stator resistance variation. The effects of dc-measurement offsets were mitigated by incorporating an integral compensating term in the observer gain. The proposed sliding-mode flux observer is capable of delivering high performance over a wide speed range, including very low speeds. Simulation results at very low speeds, including standstill and 2 r/min, without signal injection demonstrate the effectiveness of the proposed sensorless drive.

References

[1].   M. Depenbrock, "direct self-control of inverter-fed machine," ieee trans. Power electron., vol. Pe-3, no. 4. Pp. 420–429, oct. 1988.
[2].   Takahashi and t. Noguchi, "a new quick-response and high efficiency control strategy of an inductionmotor," ieee trans. Ind. Appl., vol. Ia-22, no. 5, pp. 820–827, sep./oct. 1986..
[3].   L. Zhong, m. F. Rahman, w. Y. Hu, and k. W. Lim, "analysis of direct torque control in permanent magnet synchronous motor drives," ieee trans. Power electron., vol. 12, no. 3, pp. 528–536, may 1997..
[4].   L. Tang, l. Zhong, m. F. Rahman, and y. Hu, "a novel direct torque control for interior permanent magnet synchronous machine drive system with low ripple in flux and torque and fixed switching frequency," ieee trans. Power electron., vol. 19, no. 2, pp. 346–354, mar. 2004.
[5].   D. Casadei, g. Serra, a. Stefani, a. Tani, and l. Zarri, "dtc drives for wide speed range applications using a robust flux-weakening algorithm," ieee trans. Ind. Electron., vol. 54, no. 5, pp. 2451–2461, oct. 2007.
[6].   M. Mengoni, l. Zarri, a. Tani, g. Serra, and d. Casadei, "stator flux vector control of induction motor drive in the field weakening region," ieee trans. Power electron., vol. 23, no. 2, pp. 941–949, mar. 2008.

[7]. M. Barut, s. Bogosyan, and m. Gokasan, "speed-sensorless estimation for induction motors using extended kalman filters," ieee trans. Ind. Electron., vol. 54, no. 1, pp. 272–280, feb. 2007.

[8]. M. Barut, s. Bogosyan, and m. Gokasan, "experimental evaluation of braided ekf for sensorless control of induction motors," ieee trans. Ind. Electron., vol. 55, no. 2, pp. 620–632, feb. 2008.

[9]. H.kubota, k. Matsuse, and t.nakano, "dsp based speed adaptive flux observer for induction motor applications," ieee trans. Ind. Appl., vol. 29, no. 2, pp. 344–348, mar./apr. 1993.

[10]. J. Maes and j. Melkebeek, "speed sensorless direct torque control of induction motors using an adaptive flux observer," ieee trans. Ind. Appl., vol. 35, no. 3, pp. 778–785, may/jun. 2000.

[11]. B. Nahid-mobarakeh, f. Meibody-tabar, and f.-m. Sargos, "back emf estimation-based sensorless control of pmsm: robustness with respect to measurement errors and inverter irregularities," ieee trans. Ind. Appl., vol. 43, no. 2, pp. 485–494, mar./apr. 2007.

[12]. Z. Xu and m. F. Rahman, "direct torque and flux regulation of an ipm synchronous motor drive using variable control approach," ieee trans.power. Electron., vol. 22, no. 6, pp. 2487–2498, nov. 2007.

[13]. Z. Xu and m. F. Rahman, "an adaptive sliding stator flux observer for a direct torque controlled ipm synchronous motor drive," ieee trans. Ind. Electron., vol. 54, no. 5, pp. 2398–2406, oct. 2007.

[14]. M. Rashed, p. F. A. Macconnell, a. F. Stronach, and p. Acarnley, "sensorless indirect-rotor-field-orientation speed control of a permanent magnet synchronous motor with stator resistance estimation," ieee trans. Ind. Electron., vol. 54, no. 3, pp. 1664–1675, jun. 2007.

[15]. Piippo, m. Hinkkanen, and j. Luomi, "analysis of adaptive observer for sensorless control of interior permanent magnet synchronous motors," ieee trans. Ind. Electron., vol. 55, no. 2, pp. 570–576, feb. 2008.

[16]. R. Cardenas, r. Pena, j. Clare, g. Asher, and j. Proboste, "mras observers for sensorless control of doubly-fed induction generators," ieee trans. Power electron., vol. 23, no. 3, pp. 1075–1084, may 2008.

[17]. Boldea, c. I. Pitic, c. Lascu, g.-d. Andreescu, l. Tutelea, f. Blaabjerg, and p. Sandholdt, "dtfc-svmmotion sensorless control of a pm-assisted reluctance synchronous machine as starter alternator for hybrid vehicles," ieee trans. Power electron., vol. 21, no. 3, pp. 711–719, may 2006.

[18]. N. Bianchi, s. Bolognani, j.-h. Jang, and s.-k. Sul, "comparison of pm structures and sensorless control techniques for zero-speed rotor position detection," ieee trans. Power electron., vol. 22, no. 6, pp. 2466–2475, nov. 2007.

[19]. G.-d. Andreescu, c. I. Pitic, f. Blaabjerg, and i. Boldea, "combined flux observer with signal injection enhancement for wide speed range sensorless direct torque control of ipmsm drives," ieee trans. Energy convers., vol. 23, no. 2, pp. 393–402, jun. 2008.

[20]. Khalil, s. Underwood, i. Hussain, h. Klode, b. Lequesne, s. Gopalakrishnan, and a. M. Omekanda, "four-quadrant pulse injection and sliding mode observer-based sensorless operation of a switched reluctance machine over entire speed range including zero speed," ieee trans. Ind. Electron., vol. 43, no. 3, pp. 714–723, may/jun. 2007.

[21]. Piippo, m. Hinkkanen, and j. Luomi, "signal injection in sensorless pmsm drives equipped with inverter output filter," ieee trans. Ind. Appl., vol. 44, no. 5, pp. 1614–1620, sep./oct. 2008.

[22]. S. Shinnaka, "a new speed-varying ellipse with voltage injection method for sensorless drive of permanent magnet synchronous motors with pole saliency—newpllmethod using high-frequency-current multiplied component signal," ieee trans. Ind. Appl., vol. 44, no. 3, pp. 777–788, may/jun. 2008.

[23]. G. Foo and m. F. Rahman, "sensorless sliding mode mtpa control of an ipm synchronous motor drive using a sliding mode observer and hf signal injection," ieee trans. Ind. Electron., vol. 57, no. 4, pp. 1270–1278, apr. 2010.

[24]. Boldea, m. C. Paicu, and g.-d. Andreescu, "active flux concept for motion sensorless unified ac drives," ieee trans. Power electron., vol. 23, no. 5, pp. 2612–2618, sep. 2008.

[25]. Boldea, m. C. Paicu, g.-d. Andreescu, and f. Blaabjerg, "active flux dtfc-svm sensorless control of ipmsm," ieee trans. Energy convers., vol. 24, no. 2, pp. 314–322, jun. 2009.

[26]. Boldea, m. C. Paicu, g.-d. Andreescu, and f. Blaabjerg, "active flux orientation vector sensorless control of ipmsm," in proc. Optim, may 2008, pp. 161–168.

[27]. Lascu, i. Boldea, and f. Blaabjerg, "comparative study of adaptive and inherently sensorless observers for variable-speed induction motor drives," ieee trans. Ind. Electron., vol. 53, no. 1, pp. 57–65, feb. 2006.

[28]. G. Foo and m. F. Rahman, "sensorless direct torque and flux controlled ipm synchronous motor drive at very low speed without signal injection," ieee trans. Ind. Electron., vol. 57, no. 1, pp. 395–403, jan. 2010.

[29]. J. Holtz and j.quan, "sensorless vector control of inductionmotors at very low speed using a nonlinear inverter model and parameter identification," ieee trans. Ind. Appl., vol. 38, no. 4, pp. 1087–1095, jul./aug. 2002.